J Musculoskelet Neuronal Interact 2019; 19(1):94-103

Journal of Musculoskeletal and Neuronal Interactions JMNI

Original Article

The selective TrkA agonist, gambogic amide, promotes osteoblastic differentiation and improves fracture healing in mice

Maddison R. Johnstone[1], Rhys D. Brady[1,2], Johannes A. Schuijers[1], Jarrod E. Church[1], David Orr[1], Julian M.W. Quinn[3], Stuart J. McDonald[1,*], Brian L. Grills[1,*]

[1]Department of Physiology, Anatomy and Microbiology, School of Life Sciences, La Trobe University, Melbourne, Australia;
[2]Departments of Neuroscience and Medicine, Central Clinical School, Monash University, Melbourne, Australia;
[3]Bone Research Division, Garvan Institute of Medical Research, Darlinghurst, Australia
* Joint Senior Authors

Abstract

Objectives: To study effects of the selective TrkA agonist, gambogic amide (GA), on fracture healing in mice and on an osteoprogenitor cell line *in vitro*. **Methods:** Mice were given bilateral fibular fractures and treated for two weeks with vehicle or 1 mg/kg/day GA and euthanized at 14-, 21-, and 42-days post-fracture. Calluses were analysed by micro-computed tomography (μCT), three-point bending and histology. For RT-PCR analyses, Kusa O cells were treated with 0.5nM of GA or vehicle for 3, 7, and 14 days, while for mineralization assessment, cells were treated for 21 days. **Results:** μCT analysis found that 21-day GA-treated calluses had both decreased tissue volume ($p<0.05$) and bone surface ($p<0.05$) and increased fractional bone volume ($p<0.05$) compared to controls. Biomechanical analyses of 42-day calluses revealed that GA treatment increased stiffness per unit area by 53% ($p<0.01$) and load per unit area by 52% ($p<0.01$). GA treatment increased Kusa O gene expression of alkaline phosphatase and osteocalcin ($p<0.05$) by 14 days as well as mineralization at 21 days ($p<0.05$). **Conclusions:** GA treatment appeared to have a beneficial effect on fracture healing at 21- and 42-days post-fracture. The exact mechanism is not yet understood but may involve increased osteoblastic differentiation and matrix mineralization.

Keywords: Nerve Growth Factor, TrkA Agonist, Fracture Healing, Bone

Introduction

Poor bone fracture healing is a common clinical problem that severely affects the quality of life to patients, particularly in the case of non-union (i.e., failure to join the broken bone surfaces) which frequently necessitates surgery[1-3]. Most fractures heal successfully within 2 months, but delayed and non-union fractures affect approximately 5-10% of all patients worldwide[3,4]. However, there are few non-surgical options available to improve patient outcomes and avoid non-union. One approach for identifying novel therapeutic agents that improve healing is to investigate biological mechanisms that underlie proper fracture union; such mechanisms include re-establishment of adequate blood supply and innervation of the fracture site[1,2,5,6]. In particular, it is notable that both sensory and sympathetic innervation during fracture healing improves both mineral callus composition and mechanical strength[6-8]. Nerve sprouting rapidly increases in the periosteum and callus in early stages of fracture healing, and several studies have shown that reduced fracture site innervation result in significantly larger calluses that have low bone mineral content and are consequently mechanically weaker than calluses in appropriately innervated fractures[6-11]. Accordingly, non-surgical treatments for fracture healing that increase both bone formation and innervation may improve bone healing and reduce the chance of delayed union (or non-union) of fractured bone.

The authors have no conflict of interest.

Corresponding author: Brian L Grills, Department of Physiology, Anatomy and Microbiology, La Trobe University, Melbourne, VIC, 3083, Australia
E-mail: brian.grills@latrobe.edu.au

Edited by: G. Lyritis
Accepted 18 December 2018

Nerve growth factor (NGF) is a neurotrophin responsible for growth and maintenance of sympathetic and sensory neurons in the peripheral nervous system[12], and exerts its effects via two receptors: the high-affinity/pro-growth and survival receptor TrkA, or the low-affinity/pro-apoptotic receptor, p75NTR[13,14]. Several studies in rodents have identified a beneficial role for NGF treatment in fracture healing and distraction osteogenesis, showing that topical administration of NGF increased sympathetic neurite outgrowth, accelerated the transition of immature woven bone to mature lamellar bone, increased mineralised bone within healing callus and improved mechanical properties of fractures[15-19]. Additionally, during fracture healing, both NGF and TrkA have been detected in skeletal cells, which include bone-forming osteoblasts and osteoprogenitor cells (precursor cells of osteoblasts) as well as cartilage-forming chondrocytes[20-22]. Osteoblastic MC3T3-E1 cells in an *in vitro* study also responded to NGF treatment with increased migration and greater osteoblastic differentiation, indicated by expression of alkaline phosphatase (ALP) and type 1 collagen[23]. Taken together, these findings suggest that in addition to promoting re-innervation of the fracture site, NGF may directly promote bone formation and this may enhance fracture healing.

While NGF has shown promise in pre-clinical studies, it shows poor pharmacokinetic properties, which severely limit its potential as a therapeutic agent. NGF is susceptible to proteolytic degradation and has a short elimination half-life (~2 h) following systemic administration[24-26]. Therefore, use of small, non-peptide neurotrophic mimetics may be a superior approach. Gambogic amide (GA) is a non-peptide molecule that has been shown to have selective high affinity for TrkA receptors and is tolerated *in vivo*[27-29]. Systemic administration of 2 mg/kg/day of GA in mice selectively induced TrkA activation in hippocampal neurons, reduced infarct size in a model of ischemic stroke and increased neurite outgrowth in PC12 cells[27-30]. However, to date, no studies have investigated the potential of GA treatment on fracture healing. Accordingly, we investigated the effects of GA on the structural and mechanical features of healing fractures in mice, and on osteoprogenitor cell differentiation and mineralization *in vitro*.

Methods

Animals

Eighty C57BL/6 male mice were used throughout this work and were supplied by the La Trobe University animal breeding facility. Mice were sixteen weeks of age at time of experimentation, were housed in groups of 4-5 during the experiment under a 12 h light/dark cycle and had access to food and water *ad libitum*. All experimental procedures were approved by the La Trobe University Animal Ethics Committee (AEC-13-03 and AEC 15-73), were within the guidelines of the Australian code of practice for the care and use of animals for scientific purposes by the Australian National Health and Medical Research Council, and in compliance with the ARRIVE guidelines for how to report animal experiments.

Experimental groups

All mice received bilateral fibular fractures. To assess the effects of GA (1 mg/kg/day) on fracture healing, mice were randomly assigned to receive DMSO-vehicle (controls) or GA treatment. Treatment was subcutaneously delivered via mini-osmotic pumps at a rate of 0.25 µl/h for 14 days. It has been previously shown that intraperitoneal injections of GA at doses ranging from 0.35-4 mg/kg/day resulted in increased TrkA phosphorylation in both central[29,31] and peripheral[32] neural tissues. We found that the maximum possible soluble dose of GA suitable for osmotic pump delivery was 1 mg/kg/day. Animals from treated and control groups were euthanized via carbon dioxide asphyxiation at 14-, 21-, or 42-days post-fracture.

Bilateral fibular fractures and pump insertion

Bilateral fibular fractures were conducted using previously described standard protocols[33,34]. In brief, under isoflurane anaesthesia, a 5 mm skin incision was made over the fibula. Using microtenotomy scissors, mice received a bilateral transverse and non-comminuted fibular fracture at the midpoint of the fibula approximately 12 mm proximal to the calcaneal tuberosity. Skin incisions were closed using skin glue (3M™ Vetbond™ Tissue Adhesive, St. Paul, MN, USA). Immediately post-fracture, a 10 mm incision was made on the dorsal surface of mice in between the scapulae. Mini-osmotic pumps (ALZET® Model 1002, DURECT Corporation, CA, USA) were then subcutaneously inserted and incisions were closed using Reflex wound clips.

Micro-computed tomography (µCT)

Fractured fibulae (8-11/group) were immersed in fixative (4% paraformaldehyde in 0.1 M sodium cacodylate buffer) for 48 h and then stored in 10% sucrose in 0.1 M sodium cacodylate buffer at 4°C until use. Scanning of fibulae was performed using SKYSCAN 1076 *in vivo* X-ray micro-computed tomography (Bruker-microCT) in 70% ethanol with acquisition parameters of 9 µm voxel resolution, 0.5 mm aluminium filter, 48 kV voltage, 100 µA current, 2,400 ms exposure, rotation 0.5° across 180°, frame averaging of 1. Images were reconstructed using NRecon (V1.6.3.1) with the following parameters: smoothing factor, 1; ring artefacts, 6; beam-hardening correction; 35%, pixel defect mask, 5%; C.S rotation, 0; and misalignment compensation, <3. Images were realigned and orientated using Dataviewer (V1.4.4) to obtain transaxial datasets for calluses. Analysis of the transaxial datasets was performed using CTAn (V1.11.8.0) and the region of interest (ROI) was identified as a 2 mm longitudinal region of callus (i.e. 1 mm proximal and distal to the fracture line of the callus); the border of the callus was manually traced. Thresholds used for parameter quantification were determined using

the automatic "otsu" algorithm within CTAn and visual examination of unreconstructed x-ray images. A grayscale adaptive threshold of 42-255 was used for structural analysis of calluses 14-, 21- and 42-day post-fracture. 2D and 3D data, and 3D models were generated, and the following parameters were used for structural analysis of callus: total callus volume (TV); new mineralized tissue (BV), bone fractional volume (BV/TV) and bone surface (BS).

Biomechanical assessment of fracture calluses

A three-point mechanical bending test was used to assess the effects of GA on the mechanical properties of 42-day calluses as described previously[34]. Briefly, whole fibulae with intact callus (18-20 fibulae/group) that were dissected at autopsy were stored in silicone oil at -20°C. On the day of assessment, samples were equilibrated to room temperature for 1 h. Each fibula was mounted onto the three-point bending apparatus with the callus lying centrally under the fulcrum; this ensured peak stress was applied directly in an anterior-posterior direction to the centre of each callus. A 10 N force transducer descended at a constant rate of 1.67 mm/sec and loaded each callus. Load and deflection data were recorded continuously, which plotted an x-y (load-displacement) graph. Biomechanically disrupted fracture callus ends were imprinted onto dental wax and magnified images were taken of each imprint using Leica DFC420 light microscope (Leica Microsystems Ltd., Heerbrugg, Switzerland) connected to Leica IM50 imaging software (Leica). Cross-sectional areas were obtained for each callus by averaging the total area values traced with software Leica Qwin V3 Standard (Leica). Differences in peak force to failure, load per unit area, stiffness and stiffness per unit area were calculated from the deflection data.

Histology

µCT scanned calluses were processed in LR White Resin Hard Grade Acrylic (London Resin Company, Reading, UK). Sections of un-decalcified calluses, 5 µm thick, were made longitudinally at the mid-point of the callus using a Leica RM 2155 Rotary Microtome (Leica Microsystems, Nussloch, Germany). Sections (4 per callus, 4-7 calluses/group) were histochemically stained to detect tartrate-resistant acid phosphatase (TRAP; a universal cytochemical marker for osteoclasts). Sections of callus were viewed and photographed under a Leica DFC420 light microscope (Leica). To identify whether GA treatment influenced bone resorption during fracture healing, the percentage of TRAP was measured as the total area of callus stained positive for TRAP activity divided by total callus area using Leica Qwin software (Leica) as previously described[35].

Cell culture

Kusa O cells were derived from multi-potential bone marrow stromal cells[36] and have previously been characterised as cells with osteogenic potential suitable for investigations on osteoblastic differentiation[37]. Cells were cultured in α-MEM (Gibco® Life Technologies™, Auckland, NZ), supplemented with 10% Australian Premium Foetal Bovine Serum (FBS) (Australian Ethical Biologicals Pty. Ltd., Coburg, AU), and used between passages 11-19. All cultures were maintained in an incubator at 37°C in 5% CO_2 and 95% O_2. For proliferation studies, cells were subcultured at a density of 3000 cells/ml in α-MEM supplemented with 10% FBS (α-MEM+10% FBS) for 3 h, after which medium was aspirated and replaced with α-MEM+2% FBS. Cells were treated with various concentrations of GA (0.05nM, 0.1nM, 0.5nM, 1nM, 5nM, 10nM, 50nM, 100nM, 500nM, 1µM, 5µM, 10µM) for 72 h, negative control was α-MEM only and positive controls was α-MEM+10% FBS, α-MEM + 100 ng/ml IGF (Life Technologies™, Scoresby, AU). Cell proliferation (n=4/group) was measured using CellTiter 96® AQ_{ueous} One Solution Cell Proliferation Assay kit (Promega Corporation, Madison, USA) as per manufacturer's instructions with absorbance read at 490 nm. Data was normalized to controls. For studies that required Kusa O cell differentiation, including Western blotting, RT-PCR and mineralization studies, cells were subcultured at a density of 3000 cells/ml in α-MEM + 10% FBS for 3 days, after which medium was aspirated and replaced with osteoblastic differentiation medium, which contained α-MEM+10% FBS supplemented with 50 µg/ml ascorbate and 10mM β-glycerophosphate[37,38]. Medium was replenished three days a week.

Western blotting

Lysate was isolated from undifferentiated Kusa O cells and 14 days differentiated (ascorbate/glycerophosphate exposed) Kusa O cells to analyse TrkA expression (n=6/group). Mouse brain lysates (n=2) were used as a positive control for TrkA. Briefly, cells were washed three times in PBS and then lysed in RIPA-EDTA buffer (150mM NaCl, 1% Triton X, 0.5% sodium deoxycholate, 0.1% SDS, 50mM Tris, 0.5mM EDTA) with added protease and phosphatase cocktail inhibitors. Protein sample concentration was determined using Pierce™ BCA™ Protein Assay Kit (Pierce Biotechnology, Rockford, USA), supernatant protein concentration was mixed [1:1 (v/v) ratio] with Laemmli x2 loading buffer. Samples were boiled for 5 min, centrifuged, and then stored at -20°C. Protein (10 µg) was loaded into each well and protein was separated using Precast Mini-PROTEAN® TGX™ gel (Bio-Rad Laboratories Inc., Hercules, USA). Protein bands were transferred onto polyvinyl difluoride (PVDF) membranes. The membrane was probed with anti-TrkA (1:1000, Abcam, Waterloo, NSW). Signal detection was developed with chemiluminescence (Immuno-Star™ HRP kit, Bio-Rad Laboratories Inc., Hercules, USA). Immunoreactive bands were digitally imaged using Molecular Imager® Chemidoc™ XRS+ (Bio-Rad) and results were quantified using Image Lab™ Software (Bio-Rad). Values were normalised for protein loading using α-tubulin as a loading control.

Real-time Polymerase Chain Reaction (RT-PCR)

Kusa O cells were daily cultured in osteoblastic differentiation media and treated with 0.5nM of GA or vehicle for 3, 7, and 14 days (n=5-8/group). Total RNA was prepared using PureZOL™ (Bio-Rad Laboratories Inc., Hercules, USA). RT-PCR was performed as described previously[39,40]. Briefly, reverse transcription was performed from 1 µg of total RNA using iScript™ cDNA Synthesis Kit (Bio-Rad). β-actin was used as an internal control gene. PCR was performed in triplicate using SsoFast™ EvaGreen® Supermix (Bio-Rad) and specific oligonucleotide primers (Table 1) on an iQ 96-well PCR system (Bio-Rad). Each amplification reaction contained 1 µl of cDNA and 300nM of primer. Thermal cycling conditions included initial denaturation at 95°C for 30 s, followed by 40 cycles of 95°C for 5 s and 55°C for 5 s. Melt curve analysis was performed post-cycling to confirm specificity of the amplified products. Relative quantification of genes of interest mRNA expression was determined using the $2^{-\Delta\Delta Ct}$ method.

Mineralization analysis

Kusa O cells were cultured in osteoblastic differentiating medium and treated with 0.5nM of GA or vehicle daily (n= 4/group) for 21 days[37,41]. For mineralization area analysis, Kusa O cells were washed three times in PBS, fixed in ice cold 70% ETOH for 30 min, and then stained with 0.5% Alizarin Red stain (pH 4.2) for 30 min. Cells were then washed five times in PBS and scanned images were taken. Mineralized areas were quantified using ImageJ software (National Institutes of Health, Bethesda, USA).

Statistical analysis

All outcomes were analysed using GraphPad Prism 6 software (GraphPad Software, Inc., La Jolla, USA). All data was subject to Shapiro-Wilk normality tests. All animal data outcomes and *in vitro* mineralization analysis were analysed with Mann-Whitney U tests. *In vitro* proliferation assays were analysed using regular one-way ANOVA, RT-PCR was analysed with a two-way ANOVA. Bonferroni *post-hoc* comparisons were carried out when appropriate. In all analyses, statistical significance was defined as $p<0.05$.

Results

There were no apparent behavioural changes, side effects, or changes in the weight gain pattern of GA treatment in mice.

µCT

Representative µCT reconstructions of longitudinal mid-point hemi-calluses are shown in Figure 1(a-f). Bony union was reached in all calluses by 21 days in both the GA-treated and control groups. For all µCT parameters, no effects of GA were found at either 14- or 42-days post-fracture. In contrast, analyses revealed that calluses from 21-day GA-treated mice (Figure 1g-j) had significantly reduced tissue volume (Figure 1g; $p<0.05$) which suggested a smaller callus. The measured bone surface in calluses (Figure 1j; $p<0.05$) was also lower compared to 21-day vehicle-treated mice, which suggested more consolidated bone was present in these calluses. Consistent with these observations, at 21 days post-fracture, calluses from GA-treated mice also showed increased BV/TV, i.e. bone volume fraction corrected for tissue volume (Figure 1i; $p<0.05$) compared to vehicle-treated mice.

Table 1. Oligonucleotide name and sequence (5'-3') used in Real-Time PCR.

Oligonucleotide name	Sequence (5'-3')
mBeta actin	Sense - GCTGTGCTATGTTGCTCTAG
	Anti-sense - CGCTGCTTGCCAATAGTG
mOsterix	Sense - TATGCTCCGACCTCCTCAAC
	Anti-sense - AATAAGATTGGGAAGCAGAAAG
mRunx2	Sense - AGCAACAGCAACAACAGCAG
	Anti-sense - GTAATCTGACTCTGTCCTTG
mAlkaline phosphatase	Sense - AAACCCAGACACAAGCATTCC
	Anti-sense - TCCACCAGCAAGAAGAAGCC
mOsteocalcin	Sense - TCTCTCTGACCTCACAGATCCC
	Anti-sense - TACCTTATTGCCCTCCTGCTTG
mDMP-1	Sense - CGCCGATAAGGAGGATGATG
	Anti-sense - GTGTGGTGTCTGTGGAGTC
mRANKL	Sense - ATCAGAAGACAGCACTCACT
	Anti-sense - ATCTAGGACATCCATGCTAATGT
mOsteoprotegrin	Sense - TGACCACTCTTATACGGACAG
	Anti-sense - GCCCTTCCTCACACTCAC

Biomechanical analyses

A three-point bending test was used to assess the biomechanical properties of 42-day fibular calluses. The average cross-sectional area of the fracture callus at its breaking point was significantly smaller in samples from GA-treated mice (36%, Table 2, $p<0.001$) compared to vehicle-treated mice. Calluses from GA-treated mice showed and increased load per unit area (52%) and stiffness per unit area (53%) (Table 2, $p<0.01$) compared to vehicle-treated mice. However, the peak force to failure and stiffness of calluses were not significantly different between vehicle-treated and GA-treated mice.

Histological assessment

A TRAP histochemical stain was used to assess osteoclastic density on the bone surface in calluses at 14, and 21 days post-fracture. Quantitative assessment revealed less dense TRAP histochemical staining; this was calculated as the proportion of TRAP staining/total callus surface area, in 21-day calluses compared to 14-day calluses ($p<0.01$). No

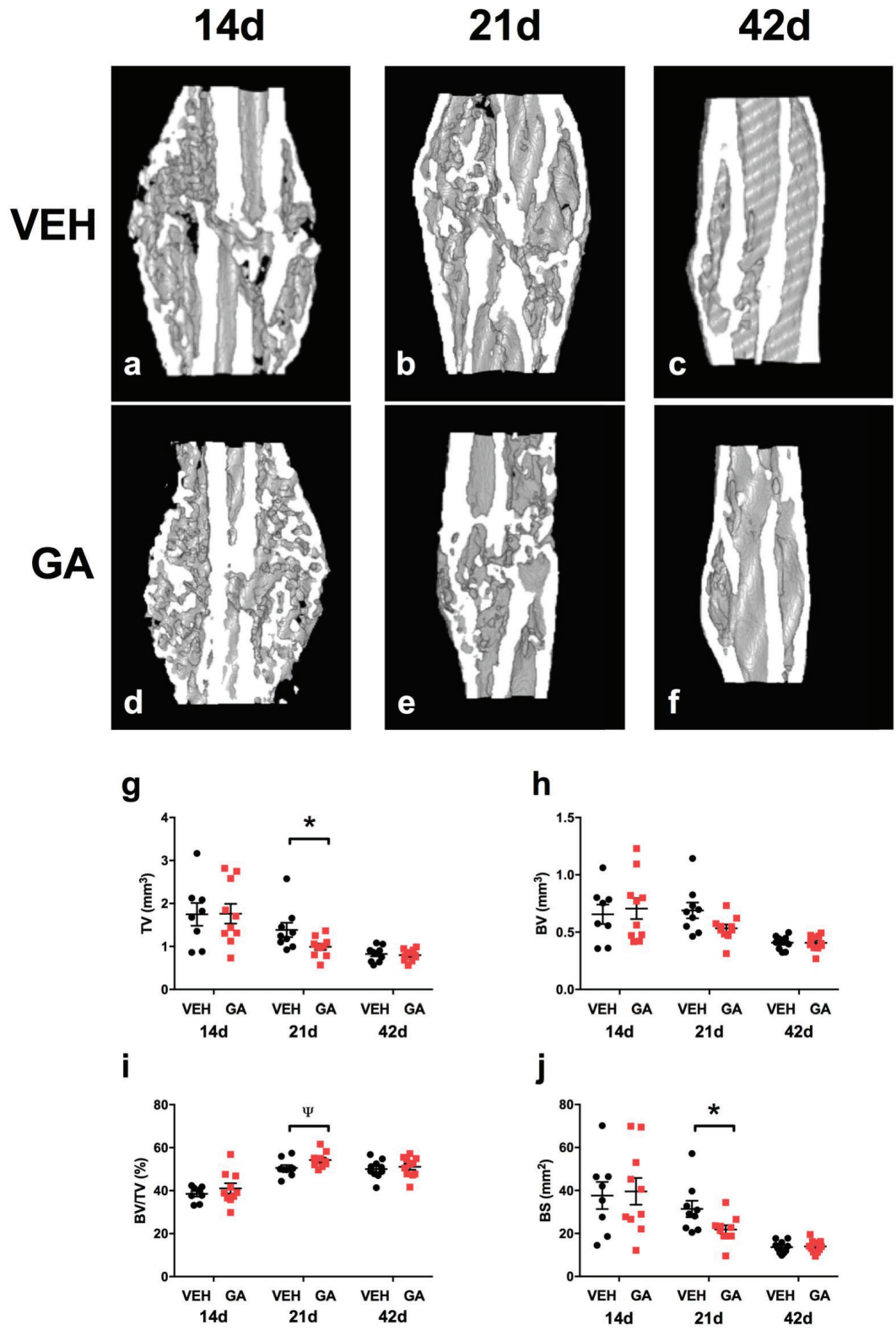

Figure 1. The effects of GA treatment on callus structural parameters using μCT. Longitudinal mid-point images representative of μCT reconstructions of hemi-calluses (a-f). μCT analysis found that GA-treated decreased callus tissue volume (g; TV) and bone surface area (j; BS) at 21 days post-fracture (*p<0.05) compared to vehicle-treated mice. There was a trend that GA increased bone fractional volume of calluses (i; Ψ p=0.05) compared to vehicle-treated mice. No differences were seen at 14-, and 42-days post-fracture between GA-treated and vehicle-treated mice. Bars are mean ± SEM, n = 8-11/group.

Table 2. Mechanical properties of control and GA-treated calluses at 42 days post-fracture.

Treatment	Peak Force (N)	Stiffness (x 10^4 Nm^2)	CSA (x 10^{-7} m^2)	LPA (x 10^7 Nm^{-2})	SPA (x 10^9 Nm^{-2})
Vehicle (n = 20) Mean ± SEM	3.92 ± 0.20	5.41 ± 0.30	5.22 ± 0.30	1.45 ± 0.13	4.15 ± 0.63
GA (n = 17) Mean ± SEM	3.76 ± 0.28	5.09 ± 0.38	3.59 ± 0.28	2.72 ± 0.43	8.63 ± 1.53
p-value	0.39	0.38	< 0.001	< 0.01	< 0.01

CSA, cross sectional area; LPA, load per unit area; SPA, stiffness per unit area. Values are means ± SEM.

differences in the percentage of TRAP staining in calluses were found between GA-treated and vehicle-treated mice, both at 14- and 21-days post-fracture (Results not shown).

Cell culture

Western blot analysis of high-affinity receptor, TrkA, was assessed in undifferentiated Kusa O cells and 14 day differentiated Kusa O cells. TrkA receptor protein expression was absent in undifferentiated Kusa O cells, however, TrkA expression was detected in 14 day differentiated Kusa O cells (Figure 2a). Proliferation assays were used to assess GA influence on Kusa O cell proliferation. At 72 h following treatment, Kusa O cell proliferation was not affected in response to daily GA-treatment ranging from 0 to 100nM. However, daily GA-treatment ranging from 500nM to 10μM significantly reduced Kusa O cell proliferation (Figure 2b, $p<0.001$) suggesting toxic effects at these doses.

RT-PCR

A pilot study on the effect of GA treatments on Kusa O differentiation *in vitro* revealed that a daily GA dose of 0.5nM appeared to increase expression of osteoblast-associated genes to a greater extent than for GA doses ranging from 1-10nM (data not shown). As such, a dose 0.5nM of GA was chosen for all further *in vitro* studies.

Kusa O cells differentiated and treated daily with 0.5nM of GA for 3, 7, and 14 days were analysed for expression of genes associated with early osteoblasts (osterix and runx2; data not shown), mature osteoblasts (ALP and osteocalcin; Figure 2c,d), osteocytes (DMP-1; Figure 2e) and osteoclastogenesis (OPG and RANKL; Figure 2f,g). Significant main effects of time and treatment, as well as an interaction were present for Kusa O expression of ALP, osteocalcin and DMP. Post-hoc analysis revealed that daily GA treatment increased the expression of ALP (Figure 2c; $p<0.01$), osteocalcin (Figure 2d; $p<0.01$) and DMP-1 (Figure 2e; $p<0.0001$) in 14-day, but not 3- and 7-day differentiated Kusa O cells compared to vehicle-treated Kusa O cells. Daily GA treatment did not influence expression of either osterix or runx2 (Data not shown). Gene expression of markers associated with osteoclastogenesis, OPG and RANKL, in Kusa O cells did not alter at 3, 7, and 14 days of differentiating or in response to daily GA treatment (Figure 2f,g).

Mineralization in vitro

Kusa O cells formed mineralised matrix during 21 days of incubation with ascorbate and β-glycerophosphate. Daily treatment of 0.5nM of GA increased mineralization area in Kusa O cells compared to control cultures (Figure 2h,i; $p<0.05$). There was no mineralisation evident in negative control cultures that employed undifferentiated Kusa O cells.

Discussion

In this study, we analysed the influence of GA, a small molecule TrkA receptor agonist during fracture healing of murine fibulae and found strong evidence that suggests GA acts in a similar manner to previously reported actions of NGF on fracture healing. GA treatment resulted in fracture calluses that were smaller in size and mechanically stronger per unit area. We showed that systemic treatment with 1 mg/kg/day GA delivered for 14 days to mice with fibular fractures decreased tissue volume of callus at 21 days post-fracture and increased the mechanical properties; load per unit area and stiffness per unit area of fractures at 42 days. Additionally, GA increased mRNA expression of markers associated with osteoblastic and osteocytic differentiation. Consistent with a direct action of GA on osteoblasts, we also found that osteoblastic differentiation and *in vitro* mineralisation was increased in osteoprogenitor Kusa O cells. Our data therefore suggests that GA, like NGF, may promote fracture healing through promoting both osteoprogenitor differentiation and mineralisation.

μCT analysis was used to determine the influence of GA on bone content of calluses at various stages during fracture healing. Of the three time-points analysed; 14, 21, and 42 days after fracture, we found significant differences in callus architecture only in the 21-day group. At 21 days post-fracture, while there was no change in the amount of bone volume, calluses of GA-treated mice had overall reduced tissue volume and elevated bone fractional volume in comparison to mice treated with vehicle, which suggests that GA treatment influenced bone remodelling of healing fractures. This finding is similar to that previously reported with NGF treatment in rats with rib fractures; where after 14 days with NGF treatment, fractured bone had smaller calluses at 21 days post-fracture[15], with enhanced bony content within

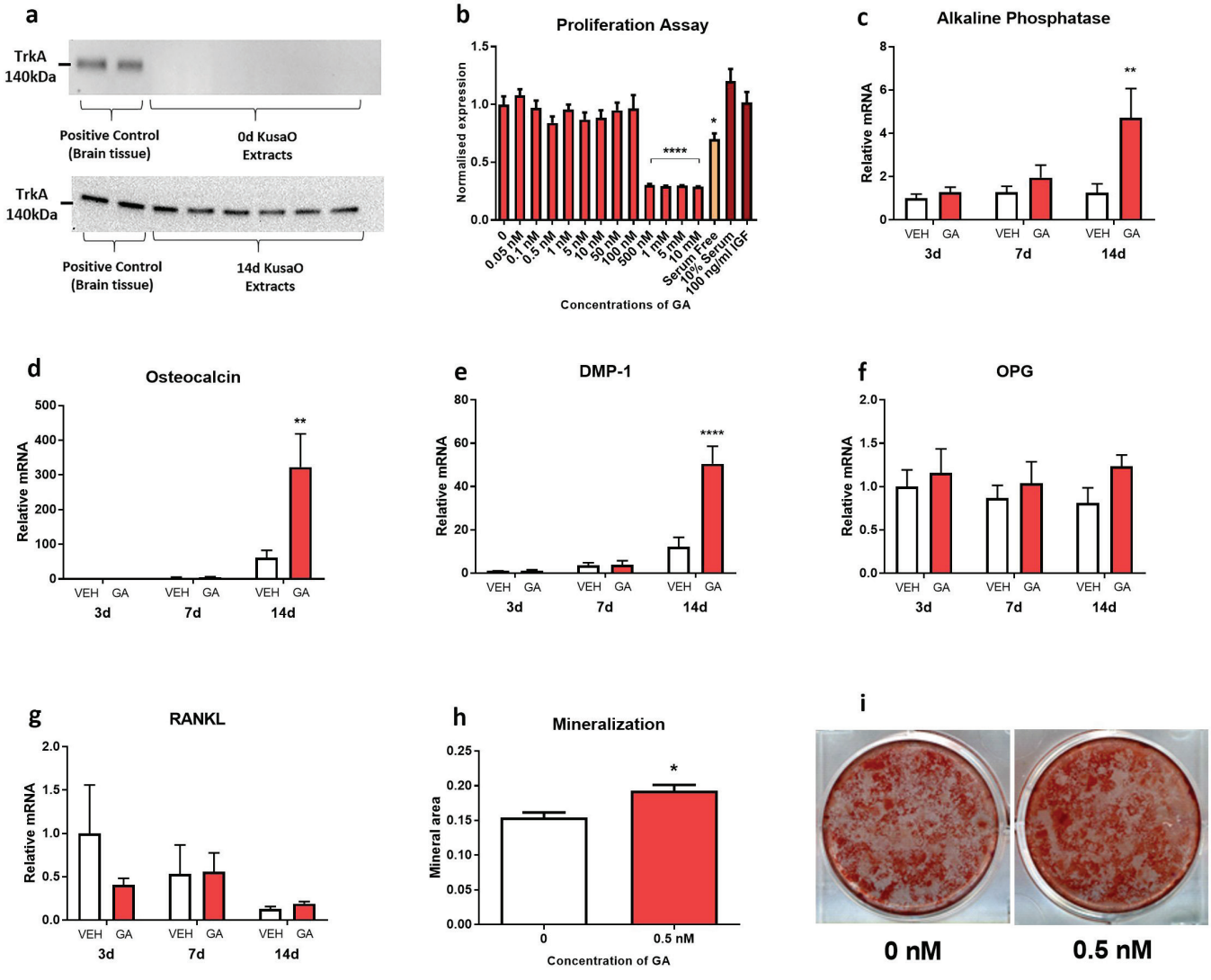

Figure 2. TrkA expression and the effects of GA treatment in the mesenchymal stem cell line, Kusa O. Western blotting (a) revealed that differentiated but not undifferentiated KusaO cells expressed TrkA. GA did not increase proliferation after 72 h of treatment, however, GA was cytotoxic at concentrations ≥500 nM (b; ****p<0.0001). Gene expression markers of mature osteoblasts (c,d), early osteocytes (e), and osteoclast formation (f,g), were analyzed at 3-, 7-, and 14-days of differentiation. GA treatment increased alkaline phosphatase (c; **p<0.01), osteocalcin (d; **p<0.01), and DMP-1 (e; ****p<0.0001) gene expression of Kusa O's at 14 days compared to vehicle. Time or GA had no effect on OPG or RANKL expression (f,g). Kusa O cells formed mineral after 21 days of incubation. GA increased mineralization of Kusa O cells compared to vehicle (h,i; *p<0.05). GA, gambogic amide; DMP-1, dentin matrix acidic phosphoprotein 1; OPG, osteoprotegrin; RANKL, receptor activator of nuclear factor kappa-B ligand. Bars are mean ± SEM, n=6-8/group.

calluses compared to vehicle-treated fractures. It is unclear whether this smaller callus trait reflected a change in cartilage formation or endochondral bone formation, however it would be consistent with a more rapid maturation of the fracture site. Several other studies involving distraction osteogenesis have also reported that NGF treatment enhanced both bone formation and callus development during the consolidation phase (28 days) of healing compared to vehicle-treated calluses[16,18,19]. One possible mechanism by which GA, like NGF, resulted in smaller calluses is likely through the stimulation of nerve growth in and around the fracture site. The periosteum of bone is densely lined with TrkA positive nerve fibres[42]. NGF treatment increased nerve growth and activity in healing rat rib calluses by upregulating catecholamine synthesis[15], which has been directly linked to stimulate both blood vessel and sensory nerve sprouting through TrkA signalling in developing endochondral bone[43]. Innervation of bone is important for angiogenesis and bone formation, which are two factors that mediate both ossification[43] and fracture healing rate[44]. It has been documented that both sensory

and sympathetic nerves within callus contribute positively in regard to fracture callus remodelling[9], with numerous studies reporting that removal of sensory and sympathetic neural input results in the formation of larger, disorganised fracture calluses[6-8]. GA, similarly to NGF, may have indirectly facilitated fracture healing by stimulating sensory and sympathetic nerve growth within the callus via TrkA, which in turn may have assisted in co-ordinating vascularisation and ossification of fractured bone to produce smaller calluses by 21 days.

Whilst our µCT data showed no differences in either tissue or bone volume of calluses by 42 days post-fracture, fracture sites from mice treated with GA had increased stiffness per unit area and load per unit area compared to vehicle-treated mice. These outcomes are identical to a previous study in our lab where NGF treatment to healing rat rib fractures improved these mechanical properties of calluses at 42 days post-fracture[15]. Nonetheless, it is important to note that GA treatment in the current study, as well as NGF treatment in the previous study[15], did not alter the mechanical properties of peak force to failure and stiffness. Mechanical strength of healing fractures is highly dependent on callus structure and degree of mineralization[45], and whilst there may not be an overall difference in the amount of bone present, there may be a difference in the quality of bone present in the callus. Our findings may indicate that there may have been a higher portion of mature, mechanically stronger lamellar bone than immature woven bone in the calluses of the GA-treated mice compared to vehicle-treated mice at 42 days, however, we were unable to distinguish the two types of bone in our µCT analysis. We postulate that this may explain why there was no difference in the amount of bone in calluses between treatments at 42 days via µCT analysis, despite the fact that biomechanically, the calluses of the GA-treated group were stronger per unit area compared to controls. Furthermore, µCT findings indicated that when compared to 21 days post-fracture, calluses at 42 days were at a substantially more advanced stage of healing in both vehicle and GA-treated groups; as such, it is possible that mechanical testing at an earlier time-point of healing (i.e. when healing was less advanced and the structural effects of GA treatment were apparent) may have yielded different findings.

Given the aforementioned findings of reduced callus size and enhanced mechanical properties, it was apparent that GA treatment caused changes to callus remodelling. TRAP staining was used to assess whether GA treatment influenced osteoclastic cell density during fracture healing, but we observed no differences in this parameter. This suggests that GA may have not influenced remodelling through bone resorption and is consistent with our *in vitro* data that showed that GA does not affect gene expression of osteoblastic OPG or RANKL, factors which together regulate osteoclastic formation and activity. Our results are supported by a recent study that reported TRAP staining density and osteoclastic number was not affected during endochondral ossification of TrkA-variant mouse pups, whereas bone formation was severely impacted, which was presumably due to the lack of NGF-TrkA signalling[43]. Additionally, other studies using immunofluorescence analysis did not find TrkA on osteoclasts, nor was this receptor found on osteoclastic precursors in callus tissue during fracture healing[20,21]. Therefore, it appears from our data that GA may not influence remodelling of calluses via osteoclastic activity and is more likely to affect bone mass in callus through promotion of osteoblastic differentiation and bone mineralisation.

To determine whether GA exerted an effect on osteoblasts and mineralisation, we utilised Kusa O cells, a murine, multi-potential bone marrow stromal cell line[36]. Undifferentiated Kusa O cells (day O) do not contain mature osteoblasts and display a phenotype that is osteoprogenitor-like[37,41]. However, by 14 days of differentiation, Kusa O cells contain many mature osteoblasts[37,41]. Through Western blotting analysis we found that the osteoblast-like Kusa O cells expressed TrkA receptors, but the undifferentiated Kusa O cells did not, which suggests that TrkA activation is more likely to occur in osteoblasts rather than osteoprogenitors in bone. This data is supported by previous reports using *in vivo* rodent models, which localised TrkA receptors in mature osteoblasts and not pre-osteoblasts during fracture healing[20-22] and suggests that TrkA signalling may be conducted via mature osteoblastic populations in bone. NGF does not influence proliferation of the murine osteoblastic precursor cell line, MC3T3-E1[23], which is consistent with our Kusa O data. Additionally, in Kusa O cells we found that GA did not influence gene expression of markers associated with early osteoblasts maturation, i.e., osterix and runx2, however, GA did increase the gene expression of markers of mature osteoblasts, namely ALP and osteocalcin, as well as the osteocytic marker, DMP-1, as well as matrix mineralisation[46,47]. Again, this is consistent with earlier studies of NGF treatment in MC3T3-E1 cells which increased ALP levels *in vitro*[23]. Furthermore, both NGF and TrkA receptor have been localised in osteoblasts during bone healing[20-22] and NGF has been shown to be important during bone formation by directly stimulating osteoblasts to synthesize bone[17,23,43].

Our findings provide evidence that GA treatment stimulated osteoblastic differentiation and mineralisation *in vitro* and improved fracture callus strength *in vivo*. The improvement in callus strength may have been, in part, due to the direct action of GA on osteoblasts, however, the possible direct action of GA on stimulating local nerves around the callus, cannot be dismissed, and this may have also contributed to improving fracture healing.

This study had some limitations. Firstly, although our findings indicate that GA had mild, positive effects on fracture healing. Due to solubility issues with osmotic pump delivery, our study was limited to use of a dosing regimen of 1 mg/kg/day. It is possible that higher doses of GA may have a more profound effect on fracture healing. Previous studies have utilised doses up to 4 mg/kg/day of GA using intraperitoneal injection[29], however osmotic pump delivery was chosen to ensure constant systemic delivery of GA. In addition, our *in vitro* findings indicate that GA may increase osteoblastic differentiation and mineralization, however quantification of

other osteoblast-associated markers and additional time-points of mineralization analysis in future studies are likely to provide further insights.

Conclusions

Our study showed that systemic administration of GA at 1 mg/kg/day for 14 days via mini-osmotic pumps in mice that were given fibular fractures had mild positive effects on fracture healing. GA treatment resulted in smaller fracture calluses with some enhancement of mechanical properties, without any detrimental side effects to the animals. Additionally, *in vitro* analysis implied that GA may act directly on osteoblasts to stimulate mineralisation. These results complement previous research and the concept that neurotrophin signalling can influence skeletal maintenance and healing.

Acknowledgements

This project was funded through the Department of Physiology, Anatomy and Microbiology at La Trobe University. No benefits in any form have been received or will be received from a commercial party related directly or indirectly to the content of this article. We would like to acknowledge laboratory technician Karen Griggs for her assistance throughout these experiments.

References

1. Hak DJ, Fitzpatrick D, Bishop JA, Marsh JL, Tilp S, Schnettler R, et al. Delayed union and nonunions: epidemiology, clinical issues, and financial aspects. Injury 2014;45(Suppl.2):S3-7.
2. Gomez-Barrena E, Rosset P, Lozano D, Stanovici J, Ermthaller C, and Gerbhard F. Bone fracture healing: cell therapy in delayed unions and nonunions. Bone 2015;70:93-101.
3. Mills LA, Simpson AH, The relative incidence of fracture non-union in the Scottish population (5.17 million): a 5-year epidemiological study. BMJ Open 2013;3(2).
4. Zura R, Xiong Z, Einhorn T, Watson JT, Ostrum RF, Prayson MJ, et al. Epidemiology of Fracture Nonunion in 18 Human Bones. JAMA Surg 2016;151(11):e162775.
5. Brinker MR, O'Connor DP. The Biological Basis for Nonunions. JBJS Rev 2016;4(6).
6. Madsen JE, Hukkanen M, Aune AK, Basran I, Moller JF, Polak JM, et al. Fracture healing and callus innervation after peripheral nerve resection in rats. Clin Orthop Relat Res 1998;(351):230-40.
7. Hukkanen M, Konttinen YT, Santavirta S, Nordsletten L, Madsen JE, Almaas R, et al. Effect of sciatic nerve section on neural ingrowth into the rat tibial fracture callus. Clin Orthop Relat Res 1995;(311):247-57.
8. Nordsletten L, Madsen JE, Almaas R, Rootwelt T, Halse J, Konttinen YT, et al. The neuronal regulation of fracture healing. Effects of sciatic nerve resection in rat tibia. Acta Orthop Scand 1994;65(3):299-304.
9. Hukkanen M, Konttinen YT, Santavirta S, Paavolainen P, Gu XH, Terenghi G, et al. Rapid proliferation of calcitonin gene-related peptide-immunoreactive nerves during healing of rat tibial fracture suggests neural involvement in bone growth and remodelling. Neuroscience 1993; 54(4):969-79.
10. Li J, Ahmad T, Spetea M, Ahmed M, Kreicbergs A. Bone reinnervation after fracture: a study in the rat. J Bone Miner Res 2001;16(8):1505-10.
11. Li J, Kreicbergs A, Bergstrom J, Stark A, Ahmed M. Site-specific CGRP innervation coincides with bone formation during fracture healing and modeling: A study in rat angulated tibia. J Orthop Res 2007;25(9):1204-12.
12. Levi-Montalcini R, Angeletti PU. Nerve growth factor. Physiol Rev 1968;48(3):534-69.
13. Micera A, Lambiase A, Stampachiacchiere B, Bonini S, Levi-Schaffer F. Nerve growth factor and tissue repair remodeling: trkA(NGFR) and p75(NTR), two receptors one fate. Cytokine Growth Factor Rev 2007;18(3-4):245-56.
14. Reichardt LF. Neurotrophin-regulated signalling pathways. Philos Trans R Soc Lond B Biol Sci 2006; 361(1473):1545-64.
15. Grills BL, Schuijers JA, Ward AR. Topical application of nerve growth factor improves fracture healing in rats. J Orthop Res 1997;15(2):235-42.
16. Cao J, Wang L, Lei DL, Liu YP, Du ZJ, Cui FZ. Local injection of nerve growth factor via a hydrogel enhances bone formation during mandibular distraction osteogenesis. Oral Surg Oral Med Oral Pathol Oral Radiol 2012;113(1):48-53.
17. Wang L, Cao J, Lei DL, Cheng XB, Zhou HZ, Hou R, et al. Application of nerve growth factor by gel increases formation of bone in mandibular distraction osteogenesis in rabbits. Br J Oral Maxillofac Surg 2010;48(7):515-9.
18. Wang L, Zhou S, Liu B, Lei D, Zhao Y, Lu C, et al. Locally applied nerve growth factor enhances bone consolidation in a rabbit model of mandibular distraction osteogenesis. J Orthop Res 2006;24(12):2238-45.
19. Letic-Gavrilovic A, Piattelli A, Abe K. Nerve growth factor beta(NGF beta) delivery via a collagen/hydroxyapatite (Col/HAp) composite and its effects on new bone ingrowth. J Mater Sci Mater Med 2003;14(2):95-102.
20. Asaumi K, Nakanishi T, Asahara H, Inoue H, Takigawa M. Expression of neurotrophins and their receptors (TRK) during fracture healing. Bone2000;26(6):625-33.
21. Grills BL, Schuijers JA. Immunohistochemical localization of nerve growth factor in fractured and unfractured rat bone. Acta Orthop Scand 1998;69(4):415-9.
22. Aiga A, Asaumi K, Lee YJ, Kadota H, Mitani S, Ozaki T, et al. Expression of neurotrophins and their receptors tropomyosin-related kinases (Trk) under tension-stress during distraction osteogenesis. Acta Med Okayama 2006;60(5):267-77.
23. Yada M, Yamaguchi K, Tsuji T. NGF stimulates differentiation of osteoblastic MC3T3-E1 cells. Biochem Biophys Res Commun 1994;205(2):1187-93.
24. Friden PM, Walus LR, Watson P, Doctrow SR, Kozarich

JW, Backman C, et al. Blood-brain barrier penetration and *in vivo* activity of an NGF conjugate. Science 1993;259(5093):373-7.
25. Tria MA, Fusco M, Vantini G, Mariot R. Pharmacokinetics of nerve growth factor (NGF) following different routes of administration to adult rats. Exp Neurol 1994; 127(2):178-83.
26. Angeletti RH, Aneletti PU, Levi-Montalcini R. Selective accumulation of (125 I) labelled nerve growth factor in sympathetic ganglia. Brain Res 1972;46:421-5.
27. Jang SW, Okada M, Sayeed I, Xiao G, Stein D, Jin P, et al. Gambogic amide, a selective agonist for TrkA receptor that possesses robust neurotrophic activity, prevents neuronal cell death. Proc Natl Acad Sci U S A 2007; 104(41):16329-34.
28. Chan CB, Liu X, Jang SW, Hsu SI, Williams I, Kang S, et al. NGF inhibits human leukemia proliferation by downregulating cyclin A1 expression through promoting acinus/CtBP2 association. Oncogene 2009; 28(43):3825-36.
29. Shen JY, Yu QS, Gambogic amide selectively upregulates TrkA expression and triggers its activation. Pharmacological Reports 2015;67(2):217-223.
30. Shah AG, Friedman MJ, Huang S, Roberts M, Li XJ, Li S. Transcriptional dysregulation of TrkA associates with neurodegeneration in spinocerebellar ataxia type 17. Hum Mol Genet 2009;18(21): 4141-52.
31. Chan CB, Liu X, Jang SW, Hsu SIH, Williams I, Kang S, et al. NGF inhibits human leukemia proliferation by downregulating cyclin A1 expression through promoting acinus/CtBP2 association. Oncogene 2009; 28(43):3825-3836.
32. Ezkurdia N, Raurell I, Rodriguez S, Gonzalez A, Esteban R, Genesca J, et al. Inhibition of Neuronal Apoptosis and Axonal Regression Ameliorates Sympathetic Atrophy and Hemodynamic Alterations in Portal Hypertensive Rats. Plos One 2014;9(1).
33. Kellum E, Starr H, Arounleut P, Immel D, Fulzele S, Wenger K, et al. Myostatin (GDF-8) deficiency increases fracture callus size, Sox-5 expression, and callus bone volume. Bone 2009;44(1):17-23.
34. Brady RD, Grills BL, Schuijers JA, Ward AR, Tonkin BA, Walsh NC, et al. Thymosin beta4 administration enhances fracture healing in mice. J Orthop Res 2014; 32(10):1277-82.
35. Brady RD, Grills BL, Church JE, Walsh NC, McDonald AC, Agoston DV, et al. Closed head experimental traumatic brain injury increases size and bone volume of callus in mice with concomitant tibial fracture. Sci Rep 2016;6:34491.
36. Umezawa A, Maruyama T, Segawa K, Shadduck RK, Waheed A, Hata J, Multipotent marrow stromal cell line is able to induce hematopoiesis *in vivo*. J Cell Physiol 1992;151(1):197-205.
37. Allan EH, Ho PW, Umezawa A, Hata J, Makishima F, Gillespie MT, et al. Differentiation potential of a mouse bone marrow stromal cell line. J Cell Biochem 2003;90(1):158-69.
38. Allan EH, Hausler KD, Wei T, Gooi JH, Quinn JM, Crimeen-Irwin B, et al. EphrinB2 regulation by PTH and PTHrP revealed by molecular profiling in differentiating osteoblasts. J Bone Miner Res 2008;23(8):1170-81.
39. Wright DK, Liu S, van der Poel C, McDonald SJ, Brady RD, Taylor L, et al. Traumatic Brain Injury Results in Cellular, Structural and Functional Changes Resembling Motor Neuron Disease. Cereb Cortex 2017;27(9):4503-4515.
40. McDonald SJ, Dooley PC, McDonald AC, Schuijers JA, Ward AR et al. Transient expression of myofibroblast-like cells in rat rib fracture callus. Acta Orthop 2012; 83(1):93-8.
41. Nakamura A, Ly C, Cipetic M, Sims NA, Vieusseux J, Kartsogiannis V, et al. Osteoclast inhibitory lectin (OCIL) inhibits osteoblast differentiation and function *in vitro*. Bone 2007;40(2):305-15.
42. Castaneda-Corral G, Jimenez-Andrade JM, Bloom AP, Taylor RN, Mantyh WG, Kaczmarska MJ, et al. The majority of myelinated and unmyelinated sensory nerve fibers that innervate bone express the tropomyosin receptor kinase A. Neuroscience 2011;178:196-207.
43. Tomlinson RE, Li Z, Zhang Q, Goh BC, Li Z, Thorek DL, et al. NGF-TrkA Signaling by Sensory Nerves Coordinates the Vascularization and Ossification of Developing Endochondral Bone. Cell Rep 2016;16(10):2723-35.
44. Beamer B, Hettrich C, Lane J. Vascular endothelial growth factor: an essential component of angiogenesis and fracture healing. HSS J 2010; 6(1):85-94.
45. Morgan EF, Mason ZD, Chien KB, Pfeiffer AJ, Barnes GL, Einhorn TA, et al. Micro-computed tomography assessment of fracture healing: relationships among callus structure, composition, and mechanical function. Bone 2009; 44(2):335-44.
46. Zhou H, Choong P, McCarthy R, Chou ST, Martin TJ, Ng KW. *In situ* hybridization to show sequential expression of osteoblast gene markers during bone formation *in vivo*. J Bone Miner Res 1994;9(9):1489-99.
47. Day TF, Guo X, Garrett-Beal L, Yang Y. Wnt/beta-catenin signaling in mesenchymal progenitors controls osteoblast and chondrocyte differentiation during vertebrate skeletogenesis. Dev Cell 2005;8(5):739-50.